Biogenic Platinum Nanoparticles' Production by Extremely Acidophilic Fe(III)-Reducing Bacteria

Matsumoto, Takahiro
Department of Earth Resources Engineering, Kyushu University

Phann, Idol
Department of Earth Resources Engineering, Kyushu University

Okibe, Naoko
Department of Earth Resources Engineering, Kyushu University

出版情報：Minerals. 11 (11), pp.1175-, 2021-10-22. MDPI
バージョン：

minerals

MDPI

Article

Biogenic Platinum Nanoparticles' Production by Extremely Acidophilic Fe(III)-Reducing Bacteria

Takahiro Matsumoto, Idol Phann and Naoko Okibe *

Department of Earth Resources Engineering, Kyushu University, 744 Motooka, Nishi-ku, Fukuoka 819-0395, Japan; conan127963302@gmail.com (T.M.); Japan; idol@mine.kyushu-u.ac.jp (I.P.)
* Correspondence: okibe@mine.kyushu-u.ac.jp

Abstract: Platinum nanoparticles (Pt(0)NPs) are expected to play a vital role in future technologies as high-performance catalysts. The microbiological route for Pt(0)NPs' production is considered a greener and simpler alternative to conventional methods. In order to explore the potential utility of extreme acidophiles, Fe(III)-reducing acidophilic bacteria, *Acidocella aromatica* and *Acidiphilium crytpum*, were tested for the production of bio-Pt(0)NPs from an acidic solution. Bio-Pt(0)NPs were successfully formed via a simple one-step reaction with the difference in the size and location between the two strains. Intact enzymatic activity was essential to exhibit the site for Pt(0) crystal nucleation, which enables the formation of well-dispersed, fine bio-Pt(0)NPs. Active *Ac. aromatica* cells produced the finest bio-Pt(0)NPs of mean and median size of 16.1 and 8.5 nm, respectively. The catalytic activity of bio-Pt(0)NPs was assessed using the Cr(VI) reduction reaction, which was shown to be in a negative linear correlation with the mean particle size under the conditions tested. This is the first study reporting the recruitment of acidophilic extremophiles for the production of Pt(0)NPs. Acidophilic extremophiles often inhabit metal-rich acidic liquors in nature and are expected to become the promising tool for metal nanotechnology.

Keywords: platinum; nanoparticles; extreme acidophiles; Fe(III)-reducing bacteria; *Acidocella* sp.; *Acidiphilium* sp.

Citation: Matsumoto, T.; Phann, I.; Okibe, N. Biogenic Platinum Nanoparticles' Production by Extremely Acidophilic Fe(III)-Reducing Bacteria. *Minerals* **2021**, *11*, 1175. https://doi.org/10.3390/min11111175

Academic Editor: Sytle M. Antao

Received: 2 September 2021
Accepted: 19 October 2021
Published: 22 October 2021

1. Introduction

Metal nanoparticles (NPs) have recently gained increasing attention owing to their potential for technological innovation in various sectors, including energy, catalysis, pharmaceuticals, optics, and photonics industries. The large specific surface area of nano-sized materials allows minimization of the metal consumption while maximizing its effect. Among other metal NPs, Pt(0)NPs are of particular importance. Their potential is widely explored in applications such as automobiles, fuel cells, petrochemicals, electronics, nanomedicine, optics, drug delivery, and antimicrobial, antioxidant, and anticancer agents [1,2]. Additionally, the production of "green" hydrogen is gaining increasing attention worldwide as an alternative clean energy to contribute to the decarbonization of the environment. "Green" hydrogen is produced via the water electrolysis reaction, wherein Pt plays a vital role as the reaction catalyst. Despite its importance and increasing demand, Pt is defined as a critical raw material and its future supply is facing concerns.

Conventionally, the production of metal NPs employs multi-step physical and chemical methods using a top-down (bulk metal is mechanically broken down to NPs) or bottom-up approach (precursor metal ions are assembled to generate NPs) [1]. However, the necessity to avoid toxic chemicals and hazardous conditions has led to an increasing interest in greener and simpler biological alternatives. So far, the biological fabrication of metal NPs explored a range of life forms, such as bacteria, yeast, fungi, algae, and plants, for metal species such Au, Ag, Pd, Pt, Ni, Co, and Fe [3,4]. The size of biogenic metal NPs can be controlled by modifying conditions such as concentrations of electron donors and reaction inhibitors [5,6].

Among those microorganisms or plants as the template for NPs' production, a number of bacterial species possess the ability to reduce soluble metal species to zero-valent nanometal. For the bio-Pt(0)NPs' production, several bacterial species have been utilized so far, e.g., *Acetobacter xylinum* [7], *Acinetobacter calcoaceticus* [8], *Desulfovibrio* spp. [9,10], *Escherichia coli* [11], *Shewanella* spp. [12,13], *Pseudomonas* spp. [14], *Streptomyces* sp. [15], and a mixed consortium of sulfate-reducing bacteria [16] as well as cyanobacteria [17,18]. In addition to whole cells, microbial cell extracts from several bacterial species have also been investigated [14]. Other than these, halophilic bacteria from salt lakes (*Halomonadaceae*, *Bacillaceae,* and *Idiomarinaceae*) were used for the production of Pt(0)NPs under acidic saline conditions (sea salt mixture and NH_4Cl, 20−210 g/L, pH 3−7) [19].

Nonetheless, despite the fact that metal-bearing solutions (metal leachates, metal-polluted waters, etc.) are often highly acidic, so far, studies on bacteriogenic Pt(0)NPs' production have focused solely on neutrophiles (or acid-tolerant halophiles). Extreme acidophiles, broadly defined as microorganisms that grow optimally at pH < 3, have potential in metal NPs' production from such highly acidic liquors but are rarely studied in this regard. Our previous studies reported the first case of bio-NPs' production of Pd(0) by extreme acidophiles, using *Acidocella (Ac.) aromatica* and *Acidiphilium (A.) crytpum*, and the extremely acidophilic archaeon, *Sulfolobus tokodaii,* from highly acidic solutions (pH 2.0–2.5), including the spent Pd catalyst leachate and at elevated Cl^- concentrations [5,20]. *Ac. aromatica* was also shown to be useful in size-controlled bio-Au(0)NPs' production [6] as well as in reducing soluble V(V) to form V(IV) precipitates in acidic liquors [21]. To the best of our knowledge, the biological synthesis of Pt(0)NPs by extreme acidophiles is not yet known. Here, we report the Pt(0)NPs' production using the two Fe(III)-reducing, extreme acidophiles, *Ac. aromatica* and *A. crytpum*.

2. Materials and Methods

2.1. Microorganisms

Ac. aromatica strain PFBC (DSM 27026^T) and *A. cryptum* strain SJH were chosen in this study as Fe(III)-reducing acidophiles which are tolerant to a number of heavy metals [22,23]. Their aerobic, heterotrophic growth can also ease the collection of cell biomass used for the following metal nanoparticles' production step. The two strains were cultivated aerobically in 500 mL Erlenmeyer flasks containing 200 mL of heterotrophic basal salts (HBS) media (per liter; 450 mg $(NH_4)_2SO_4$, 50 mg KCl, 50 mg KH_2PO_4, 500 mg $MgSO_4$ $7H_2O$, 14 mg $Ca(NO_3)_2 \cdot 4H_2O$, and 142 mg Na_2SO_4: pH 2.5 with H_2SO_4) with 0.025% (*w/v*) tryptone soya broth (TSB). Either 10 mM of fructose or 10 mM of glucose was provided as an electron donor for *Ac. aromatica* or *Acidiphilium* SJH, respectively. Flasks were incubated at 30 °C on a rotary shaker at 100 rpm.

2.2. Pt(IV) Tolerance Test

Each strain was pre-grown aerobically ($pH_{initial}$ 2.5, as described in Section 2.1), harvested at the late-exponential phase by centrifugation, washed twice, and inoculated into 15 mL test tubes containing 5 mL of fresh HBS media (pH 2.5) to the initial cell density of 1.0×10^7 cells/mL. Filter-sterilized Pt(IV) stock solution (as $H_2PtCl_6 \cdot 6H_2O$) was added to the cultures at different concentrations: 0, 0.5, 0.75, 1.0, 2.5, 5.0, or 10 mg/L. The test tubes were aerobically incubated and shaken at 100 rpm, 30 °C. Samples were regularly taken to monitor cell density (using a Thoma counting chamber). All experiments were conducted in duplicates.

2.3. Pt(IV) Reduction for Bio-Pt(0)NPs' Production

Each strain was grown aerobically (as described in Section 2.1.) until the late-exponential phase to reach the cell density of about 1.0×10^9 cells/mL. N_2 gas was purged into the culture for 3 h in order to reduce the DO (Dissolved Oxygen) level to <1.0 ppm. The N_2 gas-purged culture (100 mL) was then transferred into 100 mL vial bottles and Pt(IV) (as $H_2PtCl_6 \cdot 6H_2O$) was added to a final Pt(IV) concentration of 50 mg/L. After 1 h of incubation (to allow Pt(IV)

sorption onto the cell surface), different concentrations of sodium formate (1.0, 5.0, 10, or 20 mM, pH 2.5) were added as the sole electron donor. Sterile control cultures (with 10 or 20 mM of sodium formate) were also prepared for comparison.

In order to compare the Pt(IV) reduction behavior of active cells with or without an enzymatic inhibitor, the following comparison tests were prepared: To evaluate the effect of Cu^{2+} (as a potential enzyme inhibitor) on the Pt(IV)-reducing ability of active cells, Cu^{2+} (as $CuSO_4 \cdot 7H_2O$) was added to the media at 5 mM. All preparation after the initial aerobic cultivation was performed in an anaerobic chamber and all vial bottles were sealed with butyl rubber stoppers and aluminum crimps. The vial bottles were incubated and shaken at 100 rpm, 30 °C. Samples were regularly withdrawn using syringe needles to monitor concentrations of total Pt by the inductively coupled plasma-optical emission spectrometry (ICP-OES; Optima 8300, Perkin Elmer). All experiments were carried out in duplicate.

2.4. Characterization of Bio-Pt(0)NPs by X-ray Diffraction (XRD) and X-ray Absorption Fine Structure (XAFS)

Following the Pt(IV) reduction experiments in Section 2.3, bacterial cells were collected by centrifugation (12,000× *g*, 10 min), washed twice with fresh HBS media (pH 2.5), and freeze-dried overnight for XRD (Rigaku UltimaIV; CuKα 40 mA, 40 kV) and XAFS analyses. Cell tablets for XAFS analysis were prepared using the same amounts of cells by a tablet press machine at 10 MPa for 5 min. X-ray absorption spectra were collected with the Kyushu University beamline (BL06) at Kyushu Synchrotron Light Research Center (SAGA-LS; 1.4 GeV storage ring with a circumference of 75.6 m). The measurements were conducted at the Pt L3-edge and data were collected in fluorescence mode at the energy range from 11,300 to 12,400 eV. As standard chemicals, Pt(0) powder (Sigma-Aldrich, Tokyo, Japan: 327476) and $H_2Pt^{IV}Cl_6\ 6H_2O$ (Sigma-Aldrich, Tokyo, Japan: 206083) were used.

2.5. Ultra-Thin Section Transmission Electron Microscopy (TEM) Observation

Bacterial cells were fixed in 2.5% (*w/v*) aqueous glutaraldehyde, washed twice with phosphate buffer (pH 7.6), and then washed in 1% osmium tetroxide. Cells were dehydrated using an ethanol series (70%, 80%, 90%, and 99.5% ethanol for 5 min at each concentration, and lastly 100% dried ethanol for 10 min), washed twice in propylene oxide (5 min, twice), and finally embedded in epoxy resin (48 h, 60 °C). Sections (~70 nm) were cut with a microtome, placed onto a copper grid, and viewed with a transmission electron microscope (TEM) (TECNAI G2-20; accelerating voltage 100 kV).

2.6. Particle Size Analysis Using Image-J

Based on the ultra-thin section TEM images obtained in Section 2.5, the particle sizes of bio-Pt(0)NPs were analyzed using Image-J software (National Institute of Health, Bethesda, MD, USA). The images were calibrated and thresholded by selecting the ROI (region of interest) and removing the background noise, as appropriate. The particles were then analyzed with the "Analyze Particles" function, which calculates the projected area of an individual particle. The diameter of each particle was deduced from its projected area, assuming that the particle is spherical. Typically, over 100 particles were analyzed to calculate the average diameter and standard deviation.

2.7. Catalytic Activity of Bio-Pt(0)NPs

Bio-Pt(0)NPs were produced as described in Section 2.3. Upon the complete reduction of 50 mg/L Pt(IV) in a total of 200 mL of culture (equivalent to the formation of 10 mg of Pt(0)), bio-Pt(0)NPs were recovered by centrifugation and freeze-dried. The weight of the freeze-dried bio-Pt(0)NPs was 44.4 mg for *Ac. aromatica* and 52.0 mg for *A. cryptum* (regardless of the addition of Cu^{2+}). For the Cr(VI) reduction test, 1.0 mg of bio-Pt(0)NPs (equivalent to 0.22 mg of net-Pt(0) for *Ac. aromatica* and 0.19 mg of net-Pt(0) for *A. cryptum*) was resuspended into 20 mL of fresh HBS medium (pH 2.5) in a 20 mL vial bottle. For comparison, Pt bulk powder (≤10 μm, Sigma-Aldrich, Tokyo, Japan: 327476) and Pt/C (10 wt.% loading, matrix-activated carbon support, Sigma-Aldrich, Tokyo, Japan: 205958)

were also tested (0.2 mg of net-Pt(0) was used). Cr(VI) (as $Na_2CrO_4 \cdot 4H_2O$) and formate (as an electron donor) were then added at 10 mg/L and 10 mM, respectively. All solutions were anaerobically prepared by purging N_2 gas (<1 mg/L DO). The vial bottles were sealed with butyl rubber stoppers and incubated unshaken at 30 °C. Samples were withdrawn periodically to monitor Cr(VI) concentrations (diphenyl carbazide method [24]).

3. Results and Discussion

3.1. Effect of Pt(IV) on Bacterial Cell Growth

For the *Ac. aromatica* growth, the presence of 0.5 and 0.75 mg/L of Pt(IV) increasingly extended the lag-phase, but the final cell density was comparable to the case without Pt(IV) (~1×10^9 cells/mL). The addition of 1 mg/L of Pt(IV), however, completely inhibited the cell growth: MIC (minimal inhibitory concentration) of 1 mg/L (Figure 1a). Compared to *Ac. aromatica*, *A. cryptum* was less sensitive to Pt(IV). Although the lag-phase was largely prolonged to about 120 h, the cell density eventually reached 1×10^9 cells/mL. The presence of 5 mg/L of Pt(IV), however, was detrimental to the cell growth of *A. cryptum* (MIC of 5 mg/L; Figure 1b). According to our previous study [20], *Ac. aromatica* and *A. cryptum* had a MIC for Pd(II) at 5 mg/L (or 47 μM) and 2.5 mg/L (or 23 μM), respectively. Both strains were reported to be tolerant to high concentrations of a number of heavy metals, i.e., *Ac. aromatica* MICs at 300 mM Al^{3+}, 172 mM Fe^{2+}, 200 mM Mn^{2+}, 200 mM Ni^{2+}, 300 mM Zn^{2+}, and 5 mM Cu^{2+} [22], and *A. cryptum* MICs at >200 mM Fe^{2+}, >200 mM Fe^{3+}, and 20 mM Cu^{2+} [23]. Compared to these, platinum group metals (PGMs) such as Pd(II) and Pt(IV) were shown to be highly toxic to both strains.

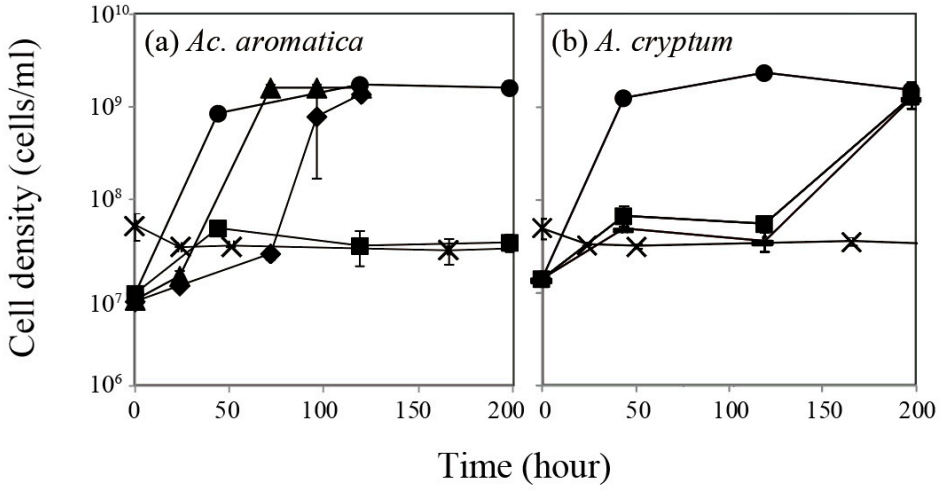

Figure 1. Effect of Pt(IV) on aerobic growth of *Ac. aromatica* (**a**) and *A. cryptum* (**b**) at $pH_{initial}$ 2.5. Initial Pt(IV) concentrations were set to 0 mg/L (●), 0.5 mg/L (▲), 0.75 mg/L (♦), 1 mg/L (■), 2.5 mg/L (—), or 5 mg/L (×). Data points are mean values from duplicate flasks.

3.2. Pt(IV) Reduction for the Production of Bio-Pt(0)NPs

Since the presence of Pt(IV) exhibited an inhibitory effect on the bacterial growth, as shown in Section 3.1, cells were pre-grown to the late-exponential phase before combining with Pt(IV) for the bio-Pt(0)NPs' production.

As shown in Figure 2, the presence of cell biomass slowed the speed of the Pt(IV) reduction reaction, compared to that in cell-free controls. Especially, active cells (without enzymatic inhibition by Cu^{2+}) showed a clear two-phase Pt(IV) reduction reaction.

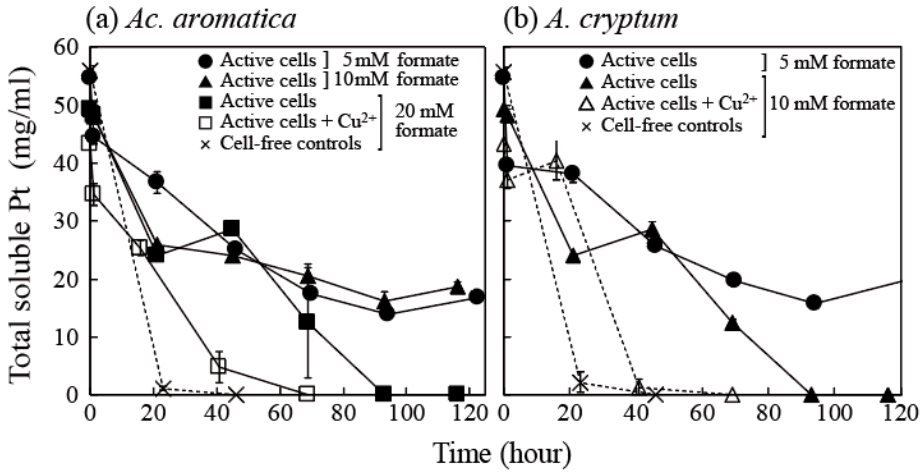

Figure 2. Pt(IV) reduction by pre-grown cells of *Ac. aromatica* (**a**) and *A. cryptum* (**b**) at $pH_{initial}$ 2.5: active cells (●, ▲, ■), active cells + 5 mM Cu^{2+} (□, △), and sterile controls (×) were compared. (**a**) Formate was added as an electron donor at 5 mM (●), 10 mM (▲), or 20 mM (■, □, ×). (**b**) Formate was added at 5 mM (●) or 10 mM (▲, △, ×). Data points are mean values from duplicate experiments.

As for the production mechanism of bio-Pt(0)NPs, Capness et al. [10] proposed the involvement of cytochromes and/or hydrogenases enzymes in anaerobic sulfate-reducing bacteria, *Desulfovibrio alaskensis*. Attard et al. [11] suggested that *E. coli* possesses various hydrogenases that catalyze the hydrogen cleavage into protons and electrons to facilitate the biogenic synthesis of Pt(0)NPs. Riddin et al. [16] proposed the involvement of two different hydrogenase enzymes in the Pt(0)NPs' production, where Pt(IV) is first reduced to Pt(II) using an oxygen-tolerant/protected novel cytoplasmic hydrogenase, followed by the second Pt(II) reduction to Pt(0)NPs by an oxygen-sensitive periplasmic hydrogenase. Additionally, the extracellular formation of Pt(0)NPs by *Streptomyces* sp. was attributed to the chloride reductase enzyme [15].

In the case of *Acidiphilium* sp. and *Acidocella* sp., the presence of putative formate dehydrogenase (FDH) enzymes is predicted from their genome sequences [25].

Sodium formate (HCOONa) added to cell suspensions existed mostly in the form of formic acid (HCOOH, pKa = 3.8) under the acidic condition used in this study. It can be hypothesized that the putative FDH enzymes decomposed formic acid to release H_2 gas (Equation (1)). H_2 gas then acted as a reducing agent for the formation of Pt(0) crystal nuclei (Equation (2)) at a number of enzymatic sites scattered over the cell surface as well as in the cytosol (Figure 3).

Platinum is a well-known chemical catalyst to accelerate Equation (1) [26]. Therefore, the two-phase Pt(IV) reduction reaction exhibited by active cells can be explained as the first slower enzymatic Pt(0) crystal nucleation phase followed by the second, faster Pt(0) crystal growth via autocatalytic Pt(IV) reduction [5,20]. In cell-free controls, the overall speed of abiotic reactions was greater but produced a few, visibly large Pt(0) aggregated particles.

In *Ac. aromatica*, the addition of 20 mM of formate resulted in the complete Pt(IV) reduction in all conditions, but with different speeds (Figure 2a). A similar trend was also observed in *A. cryptum*, but at a lower formate concentration of 10 mM (Figure 2b). This may be related to a different number of crystal nucleation sites (enzyme distribution) on active cells, as *A. cryptum* tends to form fewer NPs, as shown in this study, as well as in our previous study on bio-Pd(0)NPs [20].

$$HCOOH \rightarrow CO_2 + H_2 \quad (1)$$

$$Pt(IV) + 2H_2 \rightarrow Pt(0) + 4H^+ \quad (2)$$

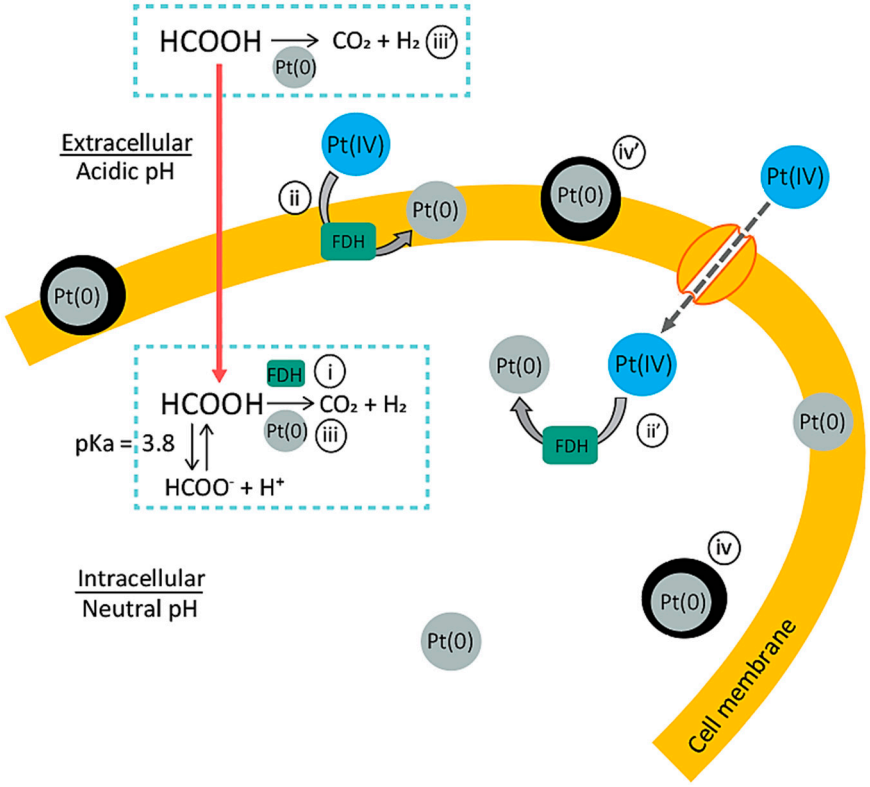

Figure 3. Proposed mechanism of the bio-Pt(0)NPs' production in active cells: (i) Formic acid (HCOOH, pKa = 3.8) existing under the acidic condition can diffuse through the cell membrane. The putative formate dehydrogenase (FDH) enzyme catalyzes the decomposition of HCOOH to CO_2 and H_2 (i). Accordingly, at each FDH site on the cell membrane (ii) and in the cytosol (ii'), Pt(IV) ions are reduced by H_2 to form the initial Pt(0) crystal nuclei (first slow reaction). Once Pt(0) nuclei are formed, Pt(0) starts to act as a chemical catalyst to accelerate the HCOOH decomposition reaction (iii). This autocatalytic reaction leads to the crystal growth of Pt(0)NPs (iv,iv') (second, faster reaction). When the corresponding enzymes are (at least partially) deactivated by Cu^{2+}, the number of crystal nucleation sites becomes limited, but the individual particle grows larger (the overall reaction time becomes shorter).

Blackish precipitates formed during the Pt(IV) reduction reaction were analyzed by XRD (Figure 4a) and XANES (Figure 4b) and confirmed to be Pt(0) particles. Cells were recovered for ultra-thin section TEM observation (Figure 5) and the following particle-size analysis (Figure 6). A number of Pt(0) particles were formed mainly on the cell surface of intact *Ac. aromatica* cells (Figure 5a,b). On the other hand, deactivating the enzymatic activity (at least partially) by Cu^{2+} resulted in the formation of larger and fewer Pt(0) particles, mainly in the cell cytosol of *Ac. aromatica* (Figure 5c). This might be due to the deactivation of membrane enzymes which are responsible for the first Pt(0) crystal nucleation step on the cell surface. Additionally, Pt(IV) might have more freely diffused through the cell membrane due to the partial loss of its selective cell permeability (owing to the cell lysis/decomposition by Cu^{2+} ions). Compared with *Ac. aromatica*, the number of bio-Pt(0)NPs formed on *A. cryptum* cells were generally lower (as was also the case with Pd(0) [20]), and scattered over the cell surface and cytosol (Figure 5d,e). The presence of Cu^{2+} ions seemingly resulted in partially disrupted cells bearing agglomerated Pt(0) particles (Figure 5f).

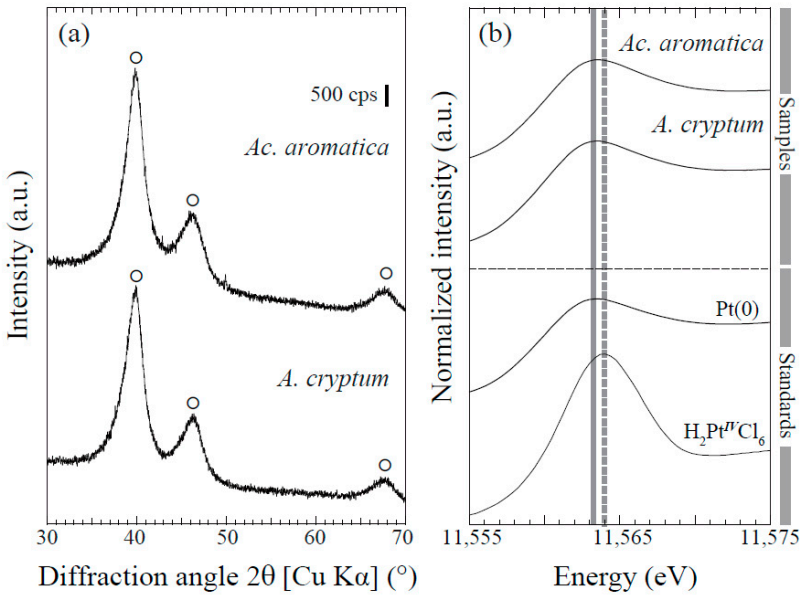

Figure 4. XRD patterns (**a**) and normalized XANES spectra at the Pt L3-edge (**b**) of bio-Pt(0)NPs produced by *Ac. aromatica* and *A. cryptum* using 20 and 10 mM of formate respectively, as an electron donor: (**a**) ○ is assigned to metallic Pt(0) (JCPDS 01-087-0640). (**b**) Grey solid and dotted lines indicate the peaks of Pt standards, Pt(0) and Pt(IV), respectively.

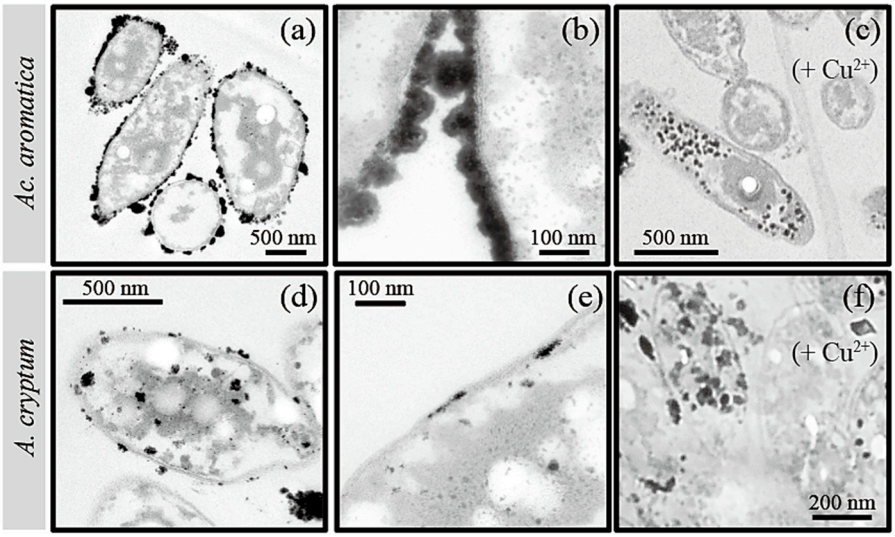

Figure 5. TEM images of bio-Pt(0)NPs produced by active cells of *Ac. aromatica* (using 20 mM of formate, (**a**–**c**)) or *A. cryptum* (using 10 mM of formate, (**d**–**f**)), without (**a**,**b**,**d**,**e**) or with (**c**,**f**) the addition of 5 mM of Cu^{2+} as a potential enzymatic inhibitor.

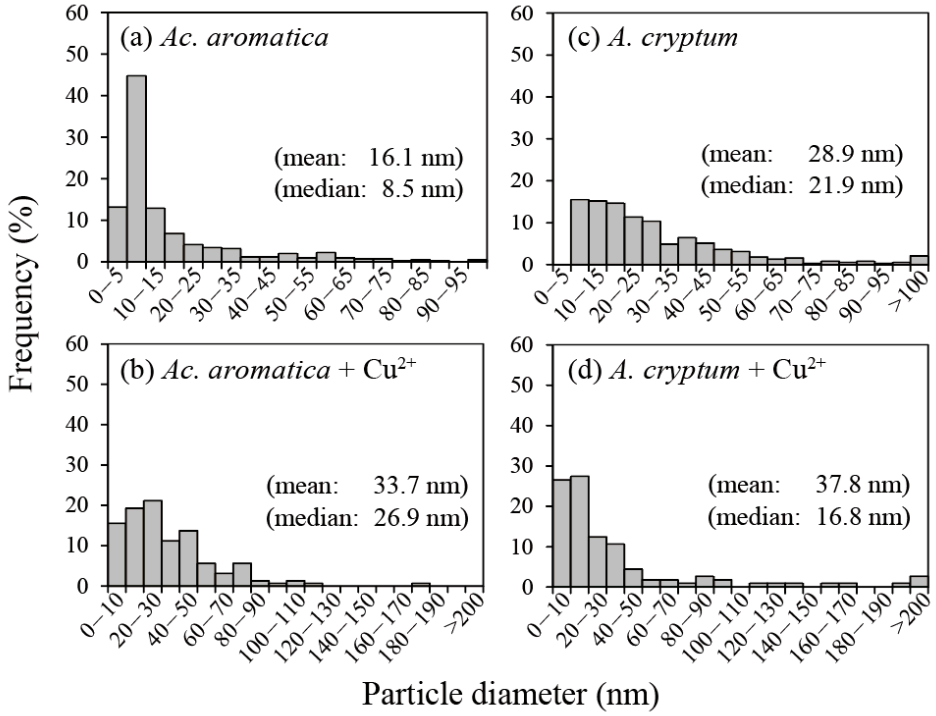

Figure 6. Particle size distributions of bio-Pt(0)NPs: (**a**,**b**) *Ac. aromatica* cells were used with 20 mM of formate. (**c**,**d**) *A. cryptum* cells were used with 10 mM of formate. (**b**,**d**) 5 mM of Cu^{2+} was added as an enzymatic inhibitor.

As was visually predicted from TEM images (Figure 5), the finest bio-Pt(0)NPs were formed by intact *Ac. aromatica* cells with the mean and median particle sizes of 16.1 and 8.5 nm respectively (Figure 6a), while bio-Pt(0)NPs formed by intact *A. cryptum* cells were in a broader size range, with the mean and median particle sizes of 28.9 and 21.9 nm, respectively (Figure 6c). The addition of an enzyme inhibitor (Cu^{2+}) resulted in the formation of larger bio-Pt(0)NPs in both *Ac. aromatica* (mean 33.7 nm, median 26.9 nm; Figure 6b) and *A. cryptum* (mean 37.8 nm, median 16.8 nm; Figure 6d).

The catalytic activity of bio-Pt(0)NPs produced under each condition was compared on the basis of the Cr(VI) reduction reaction (Equation (3)) via Equation (1).

$$Cr(VI) + 3/2H_2 \rightarrow Cr(III) + 3H^+ \quad (3)$$

Although *Ac. aromatica* originally possesses the Cr(VI) reduction capability [27], the direct microbiological effect was first eliminated by the freeze-drying treatment. As shown in Figure 7, the specific Cr(VI) reduction rate was 3.3, 1.7, 2.0, or 1.3 mg-Cr(VI)/L/h/mg-Pt(0) when bio-Pt(0)NPs produced by intact *Ac. aromatica* cells, *Ac. aromatica* cells + Cu^{2+}, intact *A. cryprum* cells, or *A. cryprum* cells + Cu^{2+} were used, respectively. This catalytic activity was in a negative linear correlation with the mean bio-Pt(0)NPs' size (Figure 7) within the condition range tested. Deactivation of the enzymatic activity by Cu^{2+} caused an appearance of outliers in the particles' distribution (larger particles of 100–200 nm or over, Figure 6c,d), which was especially noticeable with the enzyme-deactivated *A. cryptum* (Figure 6d). In fact, when the median particle size (instead of the mean particle size) was plotted, bio-Pt(0)NPs produced by the enzyme-deactivated *A. cryptum* came out of the linear correlation (data not shown). These results suggest that the catalytic activity of bio-Pt(0)NPs is largely affected by the outliers (contamination of larger particles). The presence of intact enzymatic catalysis in active cells was thus critical to act as an individual Pt(0) nucleation site, which all together enables the formation of finer and more uniform bio-Pt(0)NPs of greater catalytic activity. As a comparison, the specific Cr(VI) reduction rate by the commercially purchased Pt/C catalyst (~5 nm) was 5.7 mg-Cr(VI)/L/h/mg-Pt(0),

and was roughly on the same line with bio-Pt(0)NPs (Figure 7). The bulk Pt powder did not exhibit any Cr(VI) reduction activity and was not plotted in Figure 7.

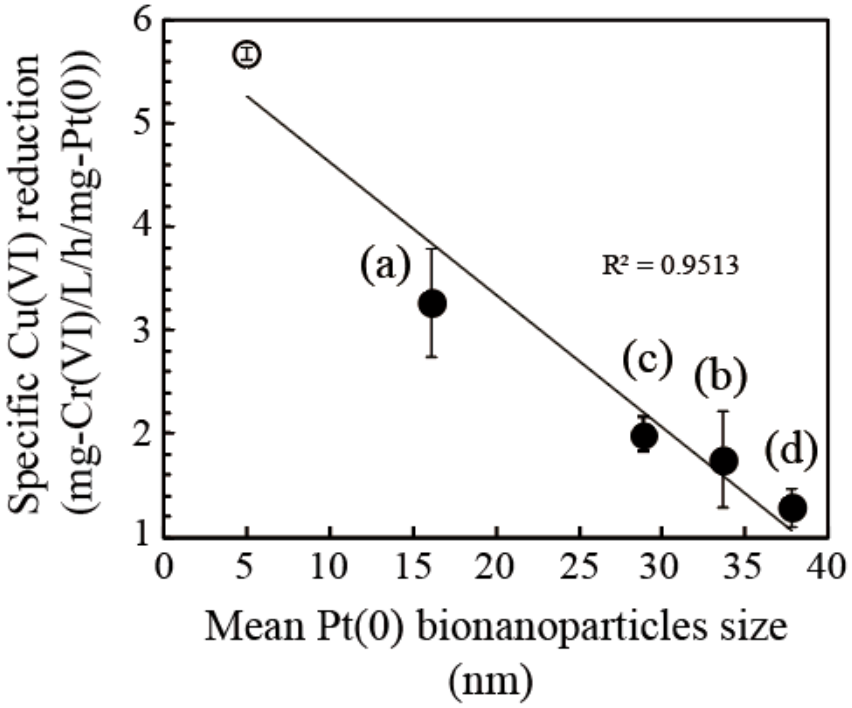

Figure 7. Catalytic activity of bio-Pt(0)NPs: Relationship between the specific Cr(VI) reduction rate (mg/L/h/mg-Pt(0)) and the mean (circles) or median (triangles) bio-Pt(0)NPs' size is shown. Bio-Pt(0)NPs (●) were produced by: (**a**) *Ac. aromatica* cells with 20 mM of formate, (**b**) *Ac. aromatica* cells with 20 mM of formate in the presence of 5 mM of Cu^{2+} as an enzymatic inhibitor, (**c**) *A. cryptum* cells with 10 mM of formate, and (**d**) *A. cryptum* cells with 10 mM of formate in the presence of 5 mM of Cu^{2+} as an enzymatic inhibitor. As a control, commercial Pt/C (Pt on carbon) was tested (○).

4. Conclusions

Bio-Pt(0)NPs were successfully produced from a highly acidic Pt(IV) solution using the extremely acidophilic Fe(III)-reducing bacteria, *Ac. aromatica* and *A. crytpum*, via a simple one-step microbiological reaction. The difference in the size and location of bio-Pt(0)NPs between the two species tested likely reflected the difference in the catalytic activity, localization, and number of the membrane proteins and enzymes responsible for Pt(0) crystal nucleation. The intact enzymatic function was critical to act as a site for Pt(0) crystal nucleation, which led to the formation of well-dispersed, fine bio-Pt(0)NPs. The finest bio-Pt(0)NPs were obtained by using intact *Ac. aromatica* cells without Cu^{2+} as an enzymatic inhibitor (mean size 16.1, median size 8.5 nm). The catalytic activity of bio-Pt(0)NPs was in a negative linear correlation with their mean particle size within the condition range tested. This is the first study reporting the acidophilic extremophiles to be used in the Pt(0)NPs' formation. Further studies on acidophilic extremophiles (especially with higher metal and salt tolerances) for biogenic metal NPs' production would benefit the development of nanobiotechnology.

Author Contributions: Conceptualization, N.O.; methodology, N.O.; validation, N.O.; formal analysis, N.O., T.M. and I.P.; investigation, T.M. and I.P.; resources, N.O.; data curation, N.O.; writing—original draft preparation, T.M. and N.O.; writing—review and editing, N.O.; visualization, T.M., I.P. and N.O.; supervision, N.O.; project administration, N.O.; funding acquisition, N.O. All authors have read and agreed to the published version of the manuscript.

Funding: This work was supported by JSPS (Japan Society for the Promotion of Science) KAKENHI, Grant Number JP16H04616 and JP20H00647.

Institutional Review Board Statement: Not applicable.

Informed Consent Statement: Not applicable.

Acknowledgments: The XAFS experiments were performed at Kyushu University Beamline (SAGA-LS/BL06: No. 2013IIK018, 2014IIK025). *Ac. aromatica* PFBC and *Acidiphilium* sp. SJH were kindly provided by D.B. Johnson (Bangor University, UK). We are grateful to Yumi Fukunaga at the Ultramicroscopy Research Center, Kyushu University, for supporting the TEM analysis.

Conflicts of Interest: The authors declare no conflict of interest.

References

1. Bönnemann, H.; Richards, R.M. Nanoscopic metal particles synthetic methods and potential applications. *Eur. J. Inorg. Chem.* **2001**, *10*, 2455–2480. [CrossRef]
2. Bloch, K.; Pardesi, K.; Satriano, C.; Ghosh, S. Bacteriogenic platinum nanoparticles for application in nanomedicine. *Front. Chem.* **2021**, *9*, 624344. [CrossRef] [PubMed]
3. Kaushik, N.; Thakkar, M.S.; Snehit, S.; Mhatre, M.S.; Rasesh, Y.; Parikh, M.S. Biological synthesis of metallic nanoparticles. *Nanomedicine* **2010**, *6*, 257–262.
4. Srivastava, S.K.; Constanti, M. Room temperature biogenic synthesis of multiple nanoparticles (Ag, Pd, Fe, Rh, Ni, Ru, Pt, Co, and Li) by *Pseudomonas aeruginosa* SM1. *J. Nanoparticle Res.* **2012**, *14*, 831. [CrossRef]
5. Kitjanukit, S.; Sasaki, K.; Okibe, N. Production of highly catalytic, archaeal Pd(0) bionanoparticles using *Sulfolobus tokodaii*. *Extremophiles* **2019**, *23*, 549–556. [CrossRef] [PubMed]
6. Rizki, I.N.; Okibe, N. Size-controlled production of gold bionanoparticles using the extremely acidophilic Fe(III)-reducing bacterium, *Acidocella aromatica*. *Minerals* **2018**, *8*, 81. [CrossRef]
7. Aritonang, H.F.; Onggo, D.; Ciptati, C.; Radiman, C.L. Synthesis of platinum nanoparticles from K_2PtCl_4 solution using bacterial cellulose matrix. *J. Nanoparticles* **2014**, *2014*, 285954. [CrossRef]
8. Gaidhani, S.V.; Yeshvekar, R.K.; Shedbalkar, U.U.; Bellare, J.H.; Chopade, B.A. Bio-reduction of hexachloroplatinic acid to platinum nanoparticles employing *Acinetobacter calcoaceticus*. *Process Biochem.* **2014**, *49*, 2313–2319. [CrossRef]
9. Martins, M.; Mourato, C.; Sanches, S.; Noronha, J.P.; Crespo, M.T.B.; Pereira, I.A.C. Biogenic platinum and palladium nanoparticles as new catalysts for the removal of pharmaceutical compounds. *Water Res.* **2017**, *108*, 160–168. [CrossRef]
10. Capeness, M.J.; Edmundson, M.C.; Horsfall, L.E. Nickel and platinum group metal nanoparticle production by *Desulfovibrio alaskensis* G20. *New Biotechnol.* **2015**, *32*, 727–731. [CrossRef]
11. Attard, G.; Casadesús, M.; Macaskie, L.E.; Deplanche, K. Biosynthesis of platinum nanoparticles by *Escherichia coli* MC4100: Can such nanoparticles exhibit intrinsic surface enantioselectivity? *Langmuir* **2012**, *28*, 5267–5274. [CrossRef]
12. Konishi, Y.; Ohnoa, K.; Saitoh, N.; Nomura, T.; Nagamine, S.; Hishida, H.; Takahashi, Y.; Uruga, T. Bioreductive deposition of platinum nanoparticles on the bacterium *Shewanella Algae*. *J. Biotechnol.* **2007**, *128*, 648–653. [CrossRef]
13. Xu, H.; Xiao, Y.; Xu, M.; Cui, H.; Tan, L.; Feng, N.; Liu, X.; Qiu, G.; Dong, H.; Xie, J. Microbial synthesis of Pd-Pt alloy nanoparticles using *Shewanella oneidensis* MR-1 with enhanced catalytic activity for nitrophenol and azo dyes reduction. *Nanotechnology* **2019**, *30*, 065607. [CrossRef] [PubMed]
14. Eramabadi, P.; Masoudi, M.; Makhdoumi, A.; Mashreghi, M. Microbial cell lysate supernatant (CLS) alteration impact on platinum nanoparticles fabrication, characterization, antioxidant and antibacterial activity. *Mater. Sci. Eng. C* **2020**, *117*, 111292. [CrossRef] [PubMed]
15. Baskaran, B.; Muthukumarasamy, A.; Chidambaram, S.; Sugumaran, A.; Ramachandran, K.; Manimuthu, T.R. Cytotoxic potentials of biologically fabricated platinum nanoparticles from *Streptomyces* sp. on MCF-7 breast cancer cells. *IET Nanobiotechnol.* **2017**, *11*, 241–246. [CrossRef]
16. Riddin, T.L.; Govender, Y.; Gericke, M.; Whiteley, C.G. Two different hydrogenase enzymes from sulphate-reducing bacteria are responsible for the bioreductive mechanism of platinum into nanoparticles. *Enzyme Microb. Technol.* **2009**, *45*, 267–273. [CrossRef]
17. Lengke, M.F.; Fleet, M.E.; Southam, G. Synthesis of platinum nanoparticles by reaction of filamentous cyanobacteria with platinum(IV)−chloride complex. *Langmuir* **2006**, *22*, 7318–7323. [CrossRef]
18. Brayner, R.; Barberousse, H.; Hemadi, M.; Djedjat, C.; Yéprémian, C.; Coradin, T.; Livage, J.; Fiévet, F.; Couté, A. Cyanobacteria as bioreactors for the synthesis of Au, Ag, Pd, and Pt nanoparticles via an enzyme-mediated route. *J. Nanosci. Nanotechnol.* **2007**, *7*, 2696–2708. [CrossRef] [PubMed]
19. Maes, S.; Props, R.; Fitts, J.P.; De Smet, R.; Vilchez-Vargas, R.; Vital, M.; Pieper, D.H.; Vanhaecke, F.; Boon, N.; Hennebel, T. Platinum recovery from synthetic extreme environments by halophilic bacteria. *Environ. Sci. Technol.* **2016**, *50*, 2619–2626. [CrossRef]
20. Okibe, N.; Nakayama, D.; Matsumoto, T. Palladium bionanoparticles production from acidic Pd(II) solutions and spent catalyst leachate using acidophilic Fe(III)-reducing bacteria. *Extremophiles* **2017**, *21*, 1091–1100. [CrossRef]
21. Okibe, N.; Maki, M.; Nakayama, D.; Sasaki, K. Microbial recovery of vanadium by the acidophilic bacterium. *Acidocella aromatica*. *Biotechnol. Lett.* **2016**, *38*, 1475–1481. [CrossRef]

22. Jones, R.M.; Hedrich, S.; Johnson, D.B. *Acidocella aromatica* sp. nov.: An acidophilic heterotrophic alphaproteobacterium with unusual phenotypic traits. *Extremophiles* **2013**, *17*, 841–850. [CrossRef]
23. Johnson, D.B.; Roberto, F.F. Heterotrophic acidophiles and their roles in the bioleaching of sulfide minerals. In *Biomining: Theory, Microbes and Industrial Processes*; Rawlings, D.E., Ed.; Springer: New York, NY, USA, 1997; pp. 259–280.
24. Noroozifar, M.; Khorasani-Motlagh, M. Specific extraction of chromium as tetrabutylammonium-chromate and spectrophotometric determination by diphenylcarbazide: Speciation of chromium in effluent streams. *Anal. Sci.* **2003**, *19*, 705–708. [CrossRef] [PubMed]
25. UniProt. Available online: http://www.uniprot.org/ (accessed on 1 September 2021).
26. Minami, Y.; Muroga, Y.; Yoshida, T.; Amao, Y. Selective hydrogen production from formate using nanoparticle with homogeneously polymer-dispersed platinum clusters. *Chem. Lett.* **2019**, *48*, 775–778. [CrossRef]
27. Masaki, Y.; Hirajima, T.; Sasaki, K.; Okibe, N. Bioreduction and immobilization of hexavalent chromium by the extremely acidophilic Fe(III)-reducing bacterium *Acidocella aromatica* strain PFBC. *Extremophiles* **2015**, *19*, 495–503. [CrossRef] [PubMed]